F. Tarpoudi Baheri,[1,2] M. Rico Luengo,[1] T. M. Schutzius,[1] D. Poulikakos,[1] and L. D. Poulikakos[3]

The Effect of Additives on Water Vapor Condensation on Bituminous Surfaces

ABSTRACT

Water condensation and freezing on asphalt roads can lead to slippery conditions, which are responsible for many winter accidents and have caused an overreliance on mostly environmentally damaging and pavement degrading deicing chemicals and salt, which requires active maintenance. Bitumen is a mechanically and chemically complex material mainly consisting of various hydrocarbon-based chemicals groups. Additionally, bitumen makes up approximately 5 wt.% of the asphalt concrete mixture because of its binder role and coating function of the aggregates, can control the bulk mechanical properties and surface properties of the asphalt mixture. Condensation as the first step and later freezing phenomena are investigated in this study and from ambient humidity toward understanding the fundamentals of icing on bituminous surfaces. Condensation experimental results show selective wettability of chemically and mechanically district bitumen surface domains. The effect of different bitumen modifiers of polyethylene terephthalate, polyamide (PA 66), polyacrylonitrile, and Sasobit wax at 1 wt.% were studied on condensation freezing and bitumen water affinity.

Introduction

Alleviating ice formation on asphalt concrete (AC) is a multibillion-dollar activity, as deicing requires time, energy, and equipment to ensure safe driving and reduce the risk of winter accidents caused by icing.[1–3] Current approaches have caused an overreliance on environmentally damaging deicing treatments. Engineering of the icephobic

surfaces enables to prevent or delay ice nucleation and lower ice normal/shear adhesion.[4,5] Most roads are bitumen-based and consist of 5 wt.% of bitumen.[6] Despite the low percentage of bitumen, the binding and coating function of the aggregates by bitumen makes bitumen surface properties one of the main parameters affecting the wettability of asphalt mixtures, also affecting related phase change upon it. Therefore, for fundamentally understanding the water interaction with bituminous surfaces, detailed analysis and studies on small scales are required.[7] Several theories and experiential techniques are used to analyze and categorize bitumen molecules, and one of the well-known approaches is to divide bitumen into four main chemical groups according to solubility, namely saturates, aromatics, resins, and asphaltenes, abbreviated as SARA fractions.[8] The colloidal system is a description of bitumen at the smallest scales and mostly responsible for rheological properties. Features at larger scales are described by the catana-peri model. Thus, the two are not mutually exclusive, but complementary at their respective scales. Because of this complex chemistry and the presence of different molecule types, the free surface of heat-cast bitumen features three main microscale domains of varying chemistry and topography.[9] Catana domain, also referred to as bee structures, are wrinkled domains that are surrounded by waxy coarse peri domains. Peri domains are also spread on the smooth neighboring para domain; however, the study and characterization of these domains is still an ongoing subject of research.[10-12] As a complex material, bitumen is composed of four main chemical groups because of their solubility, namely saturates, aromatics, resins, and asphaltenes, abbreviated as SARA fractions.[8] A variety of bitumen modifiers have been tested for their contributions to the mechanical performance of bitumen.[13-16] Among these are fibers that are either naturally abundant (e.g., cellulose) or are present in large waste quantities (e.g., polyethylene terephthalate [PET]) and modifiers, including olefinic (alkene) plastomers such as polyethylene (PE),[17] which are of interest to the present work. Polymer-modified bitumen (PMB) is now an industry standard, and it shows improved moisture resistance and higher cracking resistance at low temperatures as both unmodified and plastomer/elastomer-modified bitumen have been demonstrated to behave markedly different at freezing temperatures concerning the thermomechanical behavior.[18,19]

Water condensation rate on cold surfaces is closely tied to the wettability and hence to the hydrophobicity or water-repellency of a surface. Hydrophobicity can be influenced through several distinct but interrelated properties (a) surface patterning to obtain roughness on different length scales, (b) chemical properties that influence the surface energy of the substrate, determining the heterogeneous nucleation energy barrier and thus condensation rate.[20,21] For the surface topography effect, it has been shown that wetting interactions and droplet morphology can be tuned using surface structuring.[22] It has also been demonstrated that patterning of a surface with both hydrophobic and hydrophilic regions can influence condensation and change the nucleation energy barrier and rate.[23] Although these domains' exact chemical composition has not been unequivocally established, studies point potentially to the balance of polar asphaltenes and nonpolar waxes as making up surface domains.[10,12,24] Surface analysis showed that bitumen surface microstructures have different chemistry.[25] The surface energy (and thus intrinsic wettability) also has an effect on icephobicity, although superhydrophobic surfaces are not always icephobic, because icing also depends on nucleation thermodynamics, introducing additional complexity not always compatible with superhydrophobic structuring recipes.[26] Indeed, substrate compliance can change wetting regimes.[27] The drop-wise condensation of water on soft polymer substrates becomes especially relevant given the nature of bitumen and the variation in hardness.[28-30] Previous work has shown that by increasing the substrate compliance, the nucleation density increases, and the droplet-induced deformation of the substrate at the three-phase contact line (TPCL) can lead to a wetting ridge that possibly can prevent the merging of droplets.[31]

In this research, we modified bitumen using PET, polyamide (PA 66), polyacrylonitrile (PAN) microfibers, and commercial Sasobit wax. We then studied water condensation nucleation on different modified bitumen surfaces in comparison to virgin bitumen in cold temperatures. We aimed to understand the effect of different modifier additives on the water affinity of bitumen as a basis for understanding icing and its winter performance in future work.

Materials and Methods

BITUMEN SELECTION AND SAMPLE PREPARATION

We fabricated modified bitumen mixtures using different additives and virgin bitumen of medium softness (Q8 penetration grade 70/100, EN 1426) as the base material. First, we melted the bitumen at 137°C in an oven for 30 min. Thereafter, a speed mixer (Hauschild DAC 150.1 FVZ) was used at 2,000 rpm for 2 min, and we modified the bitumen samples adding 1 wt.% of different additives. This concentration was chosen to avoid significant changes to the mechanical properties of bitumen. The modifiers were PET, PA 66, and PAN polymer fibers, all with a diameter of 12–14 μm, and a length of 500 μm for PET (density 1.38 g/cm^3)[32] and PA 66 (density 1.15 g/cm^3), and longer PAN (density 1.184 g/cm^3) microfibers with 2,000-μm length. Sasobit wax beads (density 0.622 g/cm^3)[33] were added directly, which subsequently melted and spread homogeneously during mixing. To study the different bitumen samples under the optical microscope, we applied the modified bitumen onto commercial coverslips. We withdrew a bead of bitumen with a laboratory spatula from a few millimeters below the surface of the bulk mass of bitumen to avoid the surface layer that could be oxidized. We then spread the bitumen on commercial circular microscope coverslips (20-mm diameter) over an area of 50–150 mm^2, leading to an approximate bitumen film thickness of 0.5 mm. This was followed by annealing at 110°C on a hot plate and cooling in the refrigerator at 3°C±2°C, each time for 5 min. Samples have a thickness of several hundred micrometers, and this thickness is sufficient to avoid substrate contribution on the surface properties. Therefore, the cast bitumen samples have enough required thickness with similar surface properties to the bulk bitumen. On the other hand, as the bitumen material is thermally insulating, the several hundred-micron sample thickness shows very low thermal resistance and a more uniform temperature distribution concerning the cooling stage temperature. The virgin bitumen, which is used, has also gone over the same bitumen modification's thermal and mechanical stresses.

EXPERIMENTAL SETUP

We utilized an atomic force microscope (AFM; nanoIR2 from Bruker) in tapping mode. This device was equipped with a water coolant thermoelectric stage and used in conjunction with an environmental chamber to control the sample temperature. We purged the chamber volume with nitrogen to maintain environmentally dry conditions (RH < 3%) and prevent surface frosting at subzero temperatures. Optical microscopy was performed using an Olympus BX60 microscope. Three configuration modes were available to acquire optical images: dark field (DF), bright field, and differential interference contrast (DIC). In DF, where a ring of oblique light is projected onto the sample, the only light that has been significantly scattered can reach the centrally located objective lens. As a result, sample features of contrasting topography such as bee structures become more visible. On the other hand, DIC, which detects the phase shift of polarized light as it is reflected from the surface topography, is well suited for the other surface structures. We first recorded condensation occurrences in DF mode and then allocated the condensation sites to the different bitumen domains using the corresponding DIC images. Several studies have confirmed that optical microscopy shows the same surface topography pattern as AFM scanning images,[34,35] although not with the same resolution. Furthermore, the optical microscope equipped with a cryogenic stage (fig. 1A) provides simultaneous observation of topography and water phase change on the bitumen surface.

EXPERIMENTAL PROTOCOL

We used atomic force microscopy in a high resolution of 1,024 scan points and 1,024 lines for a square scan area of 5 by 5 μm. The scans were performed at two temperatures, 25°C and −10°C. Thereafter we analyzed the radius of curvature of the AFM topography scans with the use of a Matlab script. For brief condensation experiments under the optical microscope, samples were momentarily exposed to the humidified nitrogen stream at $T_\infty =$ 35°C ± 0.5°C and RH = 95 ± 1 %. This condition provides $P_\infty/P_{sat} = 1.6$ supersaturation condition on the sample, where the vapor pressure is P_∞, and the saturation vapor pressure at the corresponding temperature is P_{sat}. Here, it is of interest to observe the condensation of water droplets on the three main domains of bitumen: catana, peri,

Eqr {tki j v'd{ 'CUVO "ÏpvÎ*cÎ'tki j w'tgugtxgf ⁼"Y gf 'Cwi '39"36'23'WVE'42'42'42
F qy pnqcf gf Ïr tkpvgf 'd{
Nkdtct{'hqt'\j g'Tgugctej 'Ïpukwwgu'y ksj kp'g'GVJ 'Fqo ckp‹Gcy ci c .'Go r c .'RUK('Y UN‹Nkdtct{'hqt'\j g'Tgugctej 'Ïpukwwgu'y ksj kp'g'GVJ 'Fqo ckp‹Gcy ci c .'Go r c .'RUK('Y UN‹r wtuwcpv'q'Nkegpug'C

Experimental setup and bitumen surface domains. (*A*) Schematic drawing of the experimental setup and nitrogen dispensing system. (*B*) Bitumen surface under an optical microscope in DIC mode. (*C*) False colored bitumen microstructures, color code, red: catana domain, green: peri domain, remaining: para domain. Scale bars: (*B*)-(*C*) 10 μm.

and para (**fig. 1***B* and **1***C*), where the catana domain or so-called bee structure is a wrinkled domain with hills and valleys surrounded by a rough waxy peri domain, and the neighboring para domain is relatively softer than the other domains.[9] The vapor exposure experiments were repeated for the same location and sample in order to qualitatively verify the results.

In the second set of experiments, we investigated the susceptibility of supercooled condensation droplets to freezing for the different modifiers. To do so, we continually cooled the samples at −25°C/min from 25°C to −10°C (stage temperature). Immediately after reaching −10°C, another cooling rate of −1°C/min was used to cool the sample to −30°C. The initial high cooling rate was intended to minimize condensation by minimizing the droplet growth time in conditions where freezing was not expected to occur. These expectations are justified either by an insufficient degree of subcooling at above-freezing temperatures or by an insufficient latent heat release of the condensing water vapor. The second, relatively slow cooling rate of −1°C/min ensured an accurate determination of freezing temperature with a reduced thermal lag. The environmental chamber conditions at the start of each freezing trial were set to 50 % RH at 21±1°C, as measured by the built-in environmental sensors.

Results and Discussion

Here we show the surface topography development of bitumen due to cooling. **Figure 2***A* and **2***B* show the contour plots of overlaid mean surface curvature (*H*) on the height profile as a surface plot based on high-resolution AFM scans of peri and para domains at the same location. The central flat area is the para domain (see **fig. 2***A*), which is surrounded by rough peri domain at 25°C as a consequence of cooling to −10°C; both domains develop more roughness (**fig. 2***B*). The definition of the mean surface curvature *H* is given in **figure 2***C*, showing that it depends on the two principal radii of curvature R_1 and R_2. In other words, the radius of curvature is the radius of the circular arc that best fits in the normal section or combination of those on a 3D surface. Negative

Eqr {tki j v'd{ "CUVO "Kpvncrmi tkij vu'tgugtxgf =″Y gf 'Cwi "39"36 2018 no vol *Journal of Testing and Evaluation*
Fqy pnqcf gf lr tkpvgf "d{
Nkdtct{ "hqt "\j g'Tgugctej "Kpukwwgu'y ksj kp 'j g'GVJ "Fqo ckp<Gcy ci ci .'Go rc.'RUK("Y UN″Nkdtct{ "hqt "\j g'Tgugctej "Kpukwwgu'y ksj kp 'j g'GVJ "Fqo ckp<Gcy ci ci .'Go rc.'RUK("Y UN+r wtuwcpv'q'Nkegpug'C

FIG. 2 Effect of temperature on the curvature of the bitumen surface. The mean curvature (H) is overlaid on the height profile as a surface plot based on high-resolution AFM scan of peri and para domain at the same location, central flat area, is para domain surrounded by rough peri domain (A) $T = 25°C$ and (B) $T = -10°C$. (C) Schematic shows an arbitrarily curved surface in 3D, which principal radii of curvature are R_1 and R_2 projected to two perpendicular plane. (D) Histogram plots the surface area fraction occupied by surface roughness with different radius of curvature magnitudes. The para domain of the bitumen surface becomes rougher after cooling.
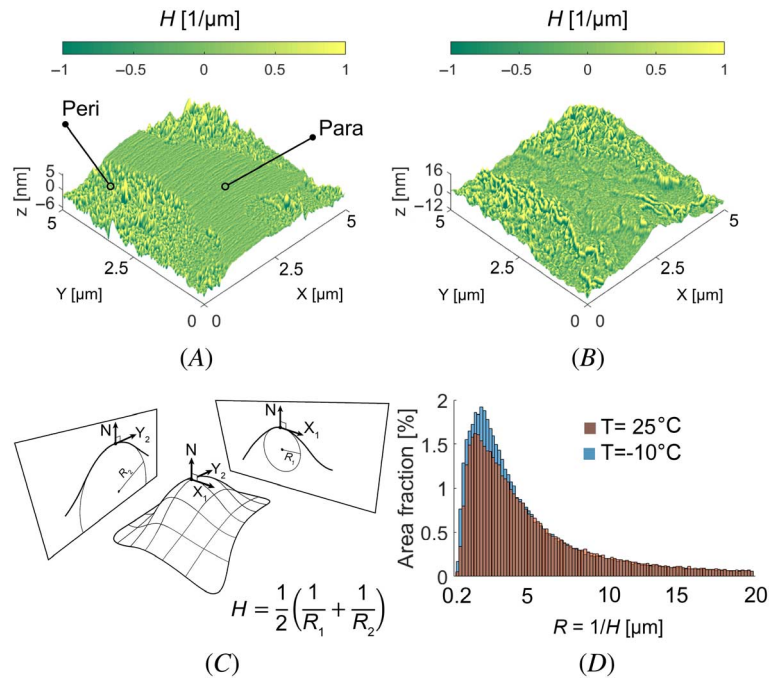
values are for concave and positive for convex curvatures. **Figure 2D** shows a histogram of the surface area fraction versus the surface radius of curvature, given by $R = 1/H$. The histogram of **figure 2D** presents the surface area coverage percentage by different radius of the curvature size magnitudes for two temperatures of 25°C and −10°C. Even though the radius of curvatures in the range of a few nanometers can boost initial condemnation and because of the AFM probe (cantilever tip) and substrate interactions and viscoelastic nature of our studied material, we could not measure surface roughness below 200 nm. Still, it can be seen that the area fraction of the smaller micro-pits increases as a function of cooling (**fig. 2D**). A more remarkable topographical evolution can be observed in the initial flat para domain than the surrounding, compared to the initially rough peri domain.

Bitumen's three main surface domains of catana, peri, and para are detectable by optical DIC image (**fig. 3A**). **Figure 3B** shows zoomed area of the selected section from **figure 3A**, and the corresponding DF image is shown in **figure 3C**. Brief condensation experiments were performed at room conditions ($T = 21±1°C$; RH = 50 %) by introducing hot vapor (at $T_\infty = 35±0.5°C$ and RH = 95±1 %) on the bitumen surface. **Figure 3D** shows a snapshot of the condensation frame. Centers of the condensed droplets are marked with white plus marks in **figure 3E** and allocated to the different domains in **figure 3F**. The analysis of more than a thousand droplet condensation sites captured for five repeatable experiments under the same conditions shows that almost 90 % of the droplets condensed on the para domain and approximately 9 % on the peri domain, and less than 1% on the catana domain (**fig. 3G**). The results were normalized with respect to the area fraction of each domain, showing the para domain remained the most favorable location for droplets to condense. Possible reasons for the observed preferential condensation could be the development of micro-pits in addition to the intrinsic differences in the surface chemistry of these two domains.

Eqr {tki j v'd{ 'CUVO "Kpv�'cml'ki j v�'tgugtxgf +='Y gf 'Cwi '39''36<47<26'GVJ 'Journal of Testing and Evaluation
F qy pmcf gf 'Ir tkpvgf 'd{
Nkdtct{ 'hqt''vj g'Tgugctej 'Kpuknwgu'y ki j kp'g'GVJ 'F qo ckp<'Gcy ci c .'Go rc .'RUK("Y UN>'Nkdtct{ 'hqt''vj g'Tgugctej 'Kpuknwgu'y ki j kp'g'GVJ 'F qo ckp<'Gcy ci c .'Go rc .'RUK("Y UN+'r wtuwcpv'q'Nkegpug'C

FIG. 3

Selective wettability of bitumen surface domains. (*A*) DIC image (X100). (*B*) Domains highlighted in colors: red: catana, green: peri, and blue: para. (*C*) Only Bee structures are visible in DF images. (*D*) Recording of droplet condensations done in DF view. (*E*) center of the condensed droplets marked by white plus marks from DF images and (*F*) overlaid concentration sites on the DIC image of the same location. (*G*) Number of condensed droplets per each specific domains (*N*) over the total count of the condensed droplets (*N*$_O$). (*H*) Normalized condensed droplet with surface area fraction of each domain (%A).
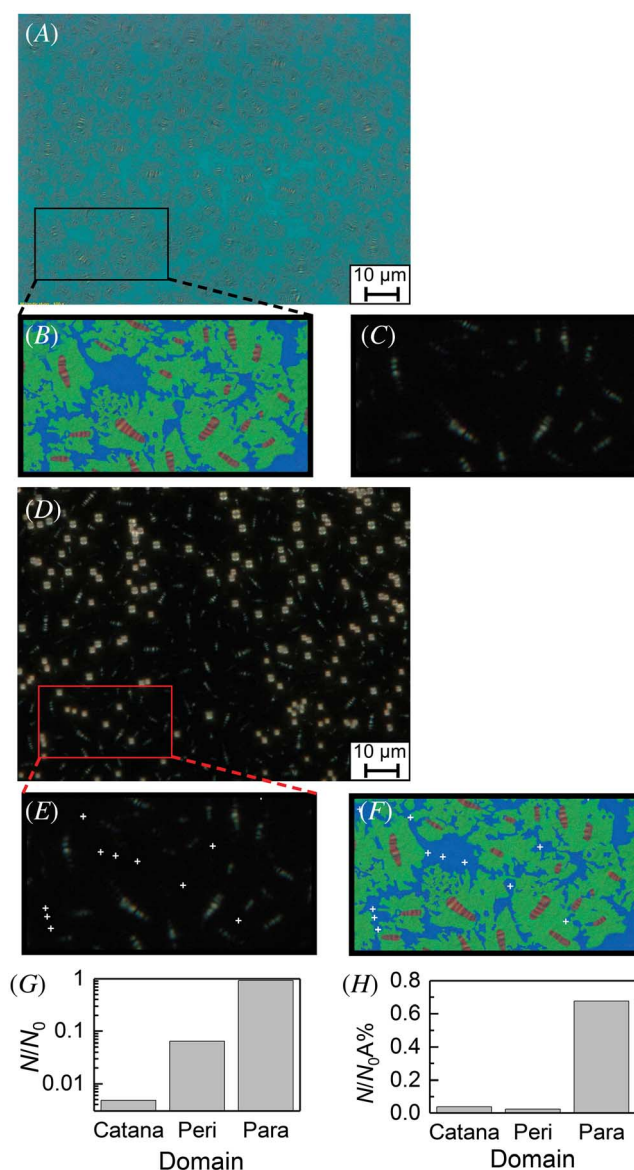

Figure 4 shows the percentage of the condensation sites relative to the bitumen surface domains. The virgin bitumen condensation results show that the para domain has the highest probability for nucleation to occur, with up to ≈ 85 %. This is in agreement with the expectation that para domains are composed of more polar para aromatic molecules with higher water affinity.[36] Also, the crystalized saturate waxes are expected to provide higher resistance to nucleation and attraction to polar substances such as water.[37] In the case of PA 66 modified bitumen, the distribution of the condensation sites in favor of the para domains is not as extreme as the other cases. Two brief condensation events ensure the validity of the results' repeatability. This is despite the possibility of small fluctuations resulting from the effects of time-varying humidity and temperature distribution on the bitumen samples. Laplace pressure, which is the pressure caused by the curved interface of gas and liquid, could accelerate this process, with water absorption in the para domain resulting in increased polarity and later

Eqr {tki j v'd{ 'CUVO "Ko],ol %cmi tki j w'tgugtxgf +="Y gf 'Cwi "39"36<32<27'424 *Journal of Testing and Evaluation*
Fqy pnqcf gf lr tkpvgf 'd{
Nkdtct{ 'hqt'\j g"Tgugctej "Kpukwwgu'y kj kp'j g''GVJ ''Fqo ckp<'Gcy ci k .''Go r c.''RUK(''Y UN''&Nkdtct{ 'hqt'\j g"Tgugctej "Kpukwwgu'y kj kp'j g''GVJ ''Fqo ckp<'Gcy ci k .''Go r c.''RUK(''Y UN''r wtuwcpv'q''Nkegpug''C

FIG. 4 Percentage of condensation sites for each respective bitumen surface domain. Condensation probability of water on four modified bitumen by PET, PA, PAN polymers or Sasobit wax at 1 wt.% concentration are compared with control virgin bitumen on samples at room condition briefly exposed to water vapor at $T_\infty = 35°C \pm 0.5°C$ and RH = 95 ± 1 %. For each of the five bitumen types, the two condensation events were repeated for three different samples, and the results normalized over the domain's area fraction to account for sample variation.
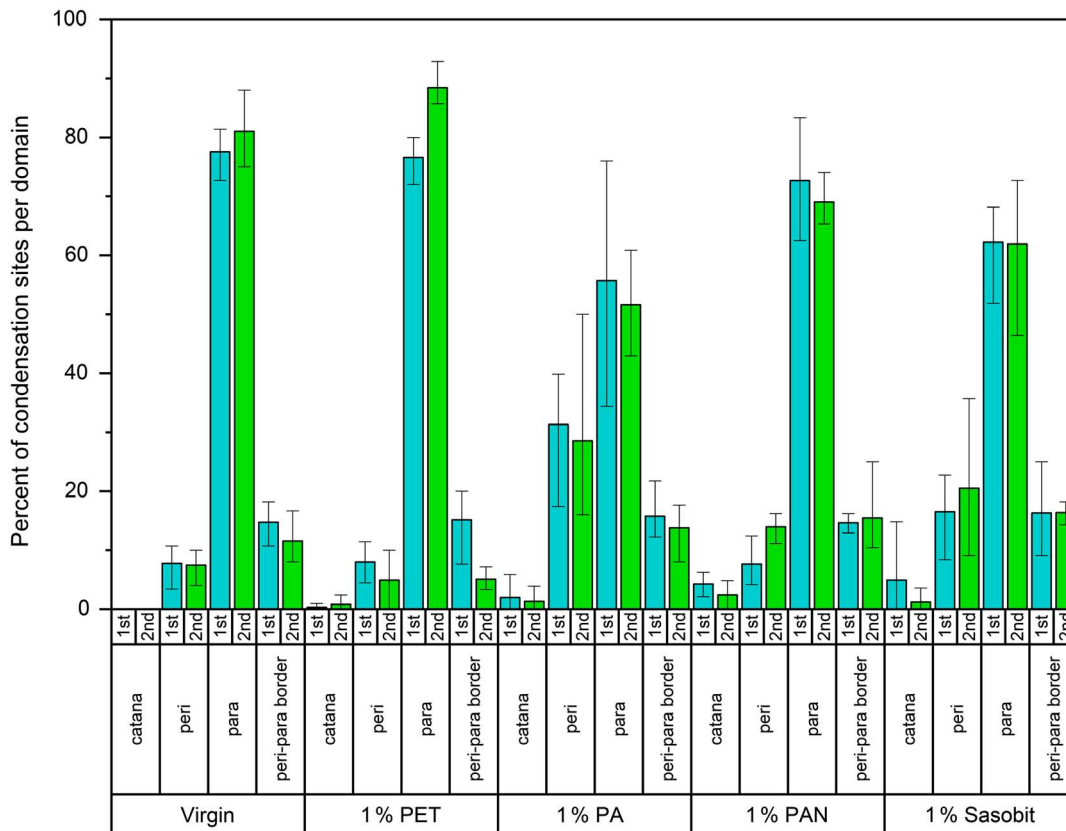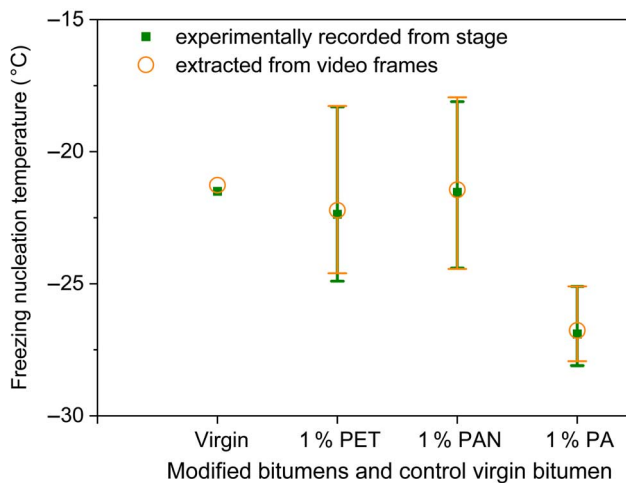

FIG. 5

Water freezing temperatures on the three modified bitumen samples and of virgin bitumen. PET, PAN, PA modified bitumens at 1 wt.% concentration are compared with control virgin bitumen on samples. The error bars indicate the minimum and maximum freezing temperatures.

condensation events causing a higher water affinity and condensation.[38] The mobility of the polar groups and the polar attraction of the condensed water would then have to be assumed to be strong enough to align the polar groups in the short time scales present and increase the surface polarity. In any case, previous research suggests that water contact with bitumen can drive the migration of asphaltenes toward the surface.[39]

We can conclude that the nucleation density is higher for the para domain in PET modified and virgin state bitumen followed by PAN, Sasobit, and PA in that order (fig. 4). PA 66 modifier shows the lowest condensation nucleation density. The polar nitrile bond of the PAN fibers could explain the high condensation nucleation density of PAN modified bitumen. Figure 5 shows the freezing nucleation temperature for the investigated materials. The results indicate that the only notable reduction in freezing temperatures was for PA 66 modified bitumen. This could be caused by an increased contact angle, which itself reduces the surface area of the drop contiguous to the substrate and lowers the condensation frequency, as reported in figure 4.

This not only lowers the probability of heterogeneous nucleation freezing but should also reduce heat transfer following the reduced extent of the TPCL. This is the topic of an ongoing investigation.

Conclusion

This study showed that the bitumen surface domains have selective wetting properties, and the surface roughness evolves at subzero temperatures. We showed that micro-scale roughness develops at cold subzero temperatures. Condensation sites were detected for four types of modified bitumen as well as unmodified, virgin bitumen. Repeated condensation also confirms that surface domains of different compositions and wetting properties keep their initial water affinity. Results show a striking difference in the bitumen domains with respect to water condensation. PA 66 modifier improves the para domain's hydrophobicity but has the opposite effect by comparison on the peri domain. A noticeable decrease in the freezing temperature was only observed for the PA 66 mixture. Further experiments on additional aspects of condensation of bituminous surfaces and their effect on frost formation are underway, and additional materials such as SBS-modified bitumen will be the subject of future investigations.

References

1. J. Andrey and R. Olley, "Relationships between Weather and Road Safety, Past and Future Research Directions," *Climatological Bulletin* 24, no. 3 (1990): 123–137.
2. Y. Yao, X. Zhao, Y. Zhang, C. Chen, and J. Rong, "Modeling of Individual Vehicle Safety and Fuel Consumption under Comprehensive External Conditions," *Transportation Research Part D Transport and Environment* 79 (January 2020): 102224, https://doi.org/10.1016/j.trd.2020.102224
3. D. L. Kelting and C. L. Laxson, "Review of Effects and Costs of Road De-icing with Recommendations for Winter Road Management in the Adirondack Park" (New York: Adirondack Watershed Institute, 2010).
4. V. Hejazi, K. Sobolev, and M. Nosonovsky, "From Superhydrophobicity to Icephobicity: Forces and Interaction Analysis," *Scientific Reports* 3 (July 2013): 2194, https://doi.org/10.1038/srep02194
5. H. C. Dan, L. H. He, J. F. Zou, L. H. Zhao, and S. Y. Bai, "Laboratory Study on the Adhesive Properties of Ice to the Asphalt Pavement of Highway," *Cold Regions Science and Technology* 104–105 (2014): 7–13, https://doi.org/10.1016/j.coldregions.2014.04.002
6. J. Read and D. Whiteoak, *The Shell Bitumen Handbook*, 5th ed. (London: Thomas Telford Ltd., 2003).
7. M. Zbik, R. G. Horn, and N. Shaw, "AFM Study of Paraffin Wax Surfaces," *Colloids and Surfaces A: Physicochemical and Engineering Aspects* 287, nos. 1–3 (September 2006): 139–146, https://doi.org/10.1016/j.colsurfa.2006.03.043
8. C. Zhang, T. Xu, H. Shi, and L. Wang, "Physicochemical and Pyrolysis Properties of SARA Fractions Separated from Asphalt Binder," *Journal of Thermal Analysis and Calorimetry* 122, no. 1 (May 2015): 241–249, https://doi.org/10.1007/s10973-015-4700-3

Eqr{tki j v'd{'CUVO"Ïpµ½ï°cmî'tki j w'tgugtxgf ±"Y gf 'Cwi'39"36¿ *Journal of Testing and Evaluation*
Fqy pnqcf gf Ïrtkpvgf'd{
Nkdtct{'hqt"\j g'Tgugctej'Ïpuwkwg u'y ksj kp'\j g'GVJ 'Fqo ckp<'Gcy ci.'Go r c.'RUK("Y UN¾ Nkdtct{'hqt"\j g'Tgugctej'Ïpuwkwg u'y ksj kp'\j g'GVJ 'Fqo ckp<'Gcy ci.'Go r c.'RUK("Y UN+'r wtuwcpv'q'Nkegpug'C

9. J.-F. Masson, V. Leblond, and J. Margeson, "Bitumen Morphologies by Phase-Detection Atomic Force Microscopy," *Journal of Microscopy* 221, no. 1 (January 2006): 17–29, https://doi.org/10.1111/j.1365-2818.2006.01540.x

10. A. M. Hung and E. H. Fini, "AFM Study of Asphalt Binder 'Bee' Structures: Origin, Mechanical Fracture, Topological Evolution, and Experimental Artifacts," *RSC Advances* 5, no. 117 (2015): 96972–96982, https://doi.org/10.1039/C5RA13982A

11. Å. L. Lyne, V. Wallqvist, M. W. Rutland, P. Claesson, and B. Birgisson, "Surface Wrinkling: The Phenomenon Causing Bees in Bitumen," *Journal of Materials Science* 48, no. 20 (June 2013): 6970–6976, https://doi.org/10.1007/s10853-013-7505-4

12. J. F. Masson, V. Leblond, J. Margeson, and S. Bundalo-Perc, "Low-Temperature Bitumen Stiffness and Viscous Paraffinic Nano- and Micro-domains by Cryogenic AFM and PDM," *Journal of Microscopy* 227, no. 3 (2007): 191–202, https://doi.org/10.1111/j.1365-2818.2007.01796.x

13. M. M. Wu, R. Li, Y. Z. Zhang, L. Fan, Y. C. Lv, and J. M. Wei, "Stabilizing and Reinforcing Effects of Different Fibers on Asphalt Mortar Performance," *Petroleum Science* 12, no. 1 (January 2015): 189–196, https://doi.org/10.1007/s12182-014-0011-8

14. T. Giuffrè, M. Morreale, G. Tesoriere, and S. Trubia, "Rheological Behaviour of a Bitumen Modified with Metal Oxides Obtained by Regeneration Processes," *Sustainability* 10, no. 3 (2018): 604, https://doi.org/10.3390/su10030604

15. M. Haq, N. Ahmad, M. Nasir, Jamal, M. Hafeez, J. Rafi, S. Zaidi, and W. Haroon, "Carbon Nanotubes (CNTs) in Asphalt Binder: Homogeneous Dispersion and Performance Enhancement," *Applied Sciences* 8, no. 12 (December 2018): 2651, https://doi.org/10.3390/app8122651

16. M. Porto, P. Caputo, V. Loise, S. Eskandarsefat, B. Teltayev, and C. Oliviero Rossi, "Bitumen and Bitumen Modification: A Review on Latest Advances," *Applied Sciences* 9, no. 4 (2019): 742, https://doi.org/10.3390/app9040742

17. J. Zhu, B. Birgisson, and N. Kringos, "Polymer Modification of Bitumen: Advances and Challenges," *European Polymer Journal* 54, no. 1 (May 2014): 18–38, https://doi.org/10.1016/j.eurpolymj.2014.02.005

18. F. Olard, H. Di Benedetto, A. Dony, and J.-C. Vaniscote, "Properties of Bituminous Mixtures at Low Temperatures and Relations with Binder Characteristics," *Materials and Structures* 38 (January 2005): 121–126, https://doi.org/10.1617/14132

19. H. R. Fischer, E. C. Dillingh, and C. G. M. Hermse, "On the Microstructure of Bituminous Binders," *Road Materials and Pavement Design* 15, no. 1 (2014): 1–15, https://doi.org/10.1080/14680629.2013.837838

20. T. M. Schutzius, S. Jung, T. Maitra, P. Eberle, C. Antonini, C. Stamatopoulos, and D. Poulikakos, "Physics of Icing and Rational Design of Surfaces with Extraordinary Icephobicity," *Langmuir* 31, no. 17 (2015): 4807–4821, https://doi.org/10.1021/la502586a

21. D. Attinger, C. Frankiewicz, A. R. Betz, T. M. Schutzius, R. Ganguly, A. Das, C.-J. Kim, and C. M. Megaridis, "Surface Engineering for Phase Change Heat Transfer: A Review," *MRS Energy & Sustainability* 1 (November 2014): 4, https://doi.org/10.1557/mre.2014.9

22. R. Enright, N. Miljkovic, A. Al-Obeidi, C. V. Thompson, and E. N. Wang, "Condensation on Superhydrophobic Surfaces: The Role of Local Energy Barriers and Structure Length Scale," *Langmuir* 28, no. 40 (August 2012): 14424–14432, https://doi.org/10.1021/la302599n

23. K. K. Varanasi, M. Hsu, N. Bhate, W. Yang, and T. Deng, "Spatial Control in the Heterogeneous Nucleation of Water," *Applied Physics Letters* 95, no. 9 (June 2009): 094101, https://doi.org/10.1063/1.3200951

24. J. N. Israelachvili, "Intermolecular and Surface Forces," in *Intermolecular and Surface Forces* (Amsterdam, the Netherlands: Elsevier, 2011), https://doi.org/10.1016/B978-0-12-391927-4.10024-6

25. F. Tarpoudi Baheri, T. M. Schutzius, D. Poulikakos, and L. D. Poulikakos, "Bitumen Surface Microstructure Evolution in Subzero Environments," *Journal of Microscopy* 279, no. 1 (March 2020): 3–15, https://doi.org/10.1111/jmi.12890

26. X. Wu, V. V. Silberschmidt, Z.-T. Hu, and Z. Chen, "When Superhydrophobic Coatings Are Icephobic: Role of Surface Topology," *Surface and Coatings Technology* 358 (January 2019): 207–214, https://doi.org/10.1016/j.surfcoat.2018.11.039

27. J. Gerber, T. Lendenmann, H. Eghlidi, T. M. Schutzius, and D. Poulikakos, "Wetting Transitions in Droplet Drying on Soft Materials," *Nature Communications* 10, no. 1 (2019): 4776, https://doi.org/10.1038/s41467-019-12093-w

28. F. Tarpoudi Baheri, L. D. Poulikakos, D. Poulikakos, and T. M. Schutzius, "Dropwise Condensation Freezing and Frosting on Bituminous Surfaces at Subzero Temperatures," *Construction and Building Materials* 298 (September 2021): 123851, https://doi.org/10.1016/j.conbuildmat.2021.123851

29. T. Vasileiou, J. Gerber, J. Prautzsch, T. M. Schutzius, and D. Poulikakos, "Superhydrophobicity Enhancement through Substrate Flexibility," *Proceedings of the National Academy of Sciences of the United States of America* 113, no. 47 (2016): 13307–13312, https://doi.org/10.1073/pnas.1611631113

30. A. Phadnis and K. Rykaczewski, "Dropwise Condensation on Soft Hydrophobic Coatings," *Langmuir* 33, no. 43 (2017): 12095–12101, https://doi.org/10.1021/acs.langmuir.7b03141

31. M. Sokuler, G. K. Auernhammer, M. Roth, C. Liu, E. Bonacurrso, and H. J. Butt, "The Softer the Better: Fast Condensation on Soft Surfaces," *Langmuir* 26, no. 3 (November 2010): 1544–1547, https://doi.org/10.1021/la903996j

32. B. Lepoittevin and P. Roger, "P. Poly(Ethylene Terephthalate)," in *Handbook of Engineering and Speciality Thermoplastics* (Hoboken, NJ: John Wiley & Sons, Inc., 2011), 97–126, https://doi.org/10.1002/9781118104729.ch4

33. M. Harooni Jamaloei, M. Aboutalebi Esfahani, and M. Filvan Torkaman, "Rheological and Mechanical Properties of Bitumen Modified with Sasobit, Polyethylene, Paraffin, and Their Mixture," *Journal of Materials in Civil Engineering* 31, no. 7 (July 2019): 04019119, https://doi.org/10.1061/(asce)mt.1943-5533.0002664

34. A. Jäger, R. Lackner, C. Eisenmenger-Sittner, and R. Blab, "Identification of Four Material Phases in Bitumen by Atomic Force Microscopy," *Road Materials and Pavement Design* 5 (2004): 9–24, https://doi.org/10.1080/14680629.2004.9689985

35. A. Ramm, N. Sakib, A. Bhasin, and M. C. Downer, "Optical Characterization of Temperature- and Composition-Dependent Microstructure in Asphalt Binders," *Journal of Microscopy* 262, no. 3 (2016): 216–225, https://doi.org/10.1111/jmi.12353

36. X. Yu, N. A. Burnham, and M. Tao, "Surface Microstructure of Bitumen Characterized by Atomic Force Microscopy," *Advances in Colloid and Interface Science* 218 (April 2015): 17–33, https://doi.org/10.1016/j.cis.2015.01.003

37. S. P. Srivastava, J. Handoo, K. M. Agrawal, and G. C. Joshi, "Phase-Transition Studies in n-Alkanes and Petroleum-Related Waxes-A Review," *Journal of Physics and Chemistry of Solids* 54, no. 6 (June 1993): 639–670, https://doi.org/10.1016/0022-3697(93)90126-C

38. A. M. Hung, A. Goodwin, and E. H. Fini, "Effects of Water Exposure on Bitumen Surface Microstructure," *Construction and Building Materials* 135 (March 2017): 682–688, https://doi.org/10.1016/j.conbuildmat.2017.01.002

39. D. Lesueur, "The Colloidal Structure of Bitumen: Consequences on the Rheology and on the Mechanisms of Bitumen Modification," *Advances in Colloid and Interface Science* 145, nos. 1–2 (2009): 42–82, https://doi.org/10.1016/j.cis.2008.08.011